

Simulation of Liquid Waves With Flow Reversal in Stratified Counter-Current Flow With a Hybrid Multi-Fluid Model

Matej Tekavčič

Reactor Engineering Division, Jožef Stefan Institute
Jamova cesta 19, SI-1000 Ljubljana, Slovenia
matej.tekavcic@ijs.si

Richard Meller, Benjamin Krull, Fabian Schlegel

Institute of Fluid Dynamics, Helmholtz-Zentrum Dresden-Rossendorf,
Bautzner Landstraße 400, 01328 Dresden, Germany
r.meller@hzdr.de, b.krull@hzdr.de, f.schlegel@hzdr.de

ABSTRACT

The present paper presents simulations of an isothermal stratified counter-current flow of air and water in a rectangular channel of the WENKA experiment (Stäbler, T.D., 2007, PhD Thesis, Univ. Stuttgart). The partial flow reversal regime with liquid waves is considered. The wavy gas-liquid surface is resolved with a hybrid multi-fluid model, featuring a consistent momentum interpolation numerical scheme, a partial elimination algorithm to handle strong drag coupling between phases, and an interface sharpening method. The Unsteady Reynolds Averaged Navier-Stokes (URANS) approach in combination with the $k-\omega$ SST (Shear Stress Transport) model and interface turbulence damping is used to model the turbulent stratified flow with wavy surface. Simulations are performed with the open source C++ library OpenFOAM. Results are validated with experimental data for the height of liquid surface, profiles of velocity and of turbulent kinetic energy, and the amount of reversed liquid flow.

1 INTRODUCTION

Processes involving gas-liquid flows are important for reliable, efficient and safe operation of many industrial applications, such as electricity generation in nuclear power plants. Many different two-phase flow patterns can appear in these systems, with a wide range of scales considering both interfacial and turbulent structures. Stratified flow, i.e. phases being separated by a smooth or wavy interface, is one of the most important regimes for safety analyses.

During a hypothetical loss-of-coolant accident in a pressurized water reactor, safety concerns during cold water injection of the emergency core cooling system include: significant stress on the primary components due to pressurized thermal shock [1], possible formation of condensation-induced water hammer [2], and occurrence of the counter-current flow limitation [3], among others. Comprehensive knowledge of turbulent flow conditions near the stratified gas-liquid interface is important for the analyses of the aforementioned phenomena. In that context, computational fluid dynamics (CFD) simulations represent an important complementary research and analytical tool, as the experimental observation of industrial turbulent multiphase flows can be challenging.

Due to limited computational power, using precise interface tracking methods to resolve all relevant physical scales and flow morphologies in complex unsteady multiphase flows (including surface waves, slugs, bubbles and droplets, etc.) is unfeasible for larger industrial applications, such as real nuclear reactors. In these cases, the less accurate two-fluid models, based on the concept of phase averaging, and Unsteady Reynolds Averaged Navier-Stokes (URANS) turbulence modelling are the more practical approach in terms of computational effort. As such tools are developed to simulate dispersed flows, where individual positions of small bubble interfaces are lost due to averaging, additional methods are required to model the larger, numerically resolvable gas-liquid interface in the stratified flow regime.

OpenFOAM-Hybrid [4, 5] is an advanced two-fluid model based simulation tool for multiphase flows developed in the open-source CFD library OpenFOAM. Hybrid models combine multiple specialised methods covering different particular flow regimes, as it is desirable to reproduce complex two-phase phenomena within a single, comprehensive computational tool.

The objective of the present study is to show the capability of the hybrid model to simulate turbulent counter-current stratified flow in the partial flow reversal regime with significant liquid waves. The focus is on evaluating the interface turbulence damping method used to improve the description of the flow near a gas-liquid surface in the URANS modelling approach. Simulation results are validated with the measurement data from the WENKA experiment [6].

2 NUMERICAL SIMULATION

2.1 Hybrid model equations

Isothermal two-phase flow of incompressible air and water without phase change is considered in the present work. The hybrid simulation model [4] is based on phase averaged continuity and momentum equations of the two-fluid model [7] written for each phase α as

$$\frac{\partial r_\alpha}{\partial t} + \mathbf{u}_\alpha \cdot \nabla r_\alpha = 0, \quad (1)$$

$$\frac{\partial (r_\alpha \rho_\alpha \mathbf{u}_\alpha)}{\partial t} + \nabla \cdot (r_\alpha \rho_\alpha \mathbf{u}_\alpha \mathbf{u}_\alpha) = \nabla \cdot \mathbf{T}_\alpha - r_\alpha \nabla p + r_\alpha \rho_\alpha \mathbf{g} + \mathbf{F}_{\alpha\beta}^\sigma + \mathbf{F}_{\alpha\beta}^D, \quad (2)$$

where r_α , ρ_α , \mathbf{u}_α are the volume fraction, density and velocity field of phase α , respectively. The effective stress tensor \mathbf{T}_α combines viscous and turbulent stresses. The latter is calculated using the k - ω SST turbulence model [8]. A single pressure field p is shared between phases. Effects of buoyancy are taken into account with the $r_\alpha \rho_\alpha \mathbf{g}$ term, where $\mathbf{g} = (0, -g, 0)$ is the acceleration of gravity in negative y direction. The continuum surface force model [9] is used to model the surface tension force $\mathbf{F}_{\alpha\beta}^\sigma$ between the phases α and β . A constant surface tension coefficient is prescribed for air and water with $\sigma = 0.072$ N/m.

In the present work, the wavy gas-liquid surface is assumed as (numerically) well resolved, which presupposes there is no slip between individual phase velocities at the interface. Such Volume-of-Fluid-like behaviour of the hybrid model is achieved with the strong momentum coupling term imposed by the numerical drag force [10] defined as

$$\mathbf{F}_{\alpha\beta}^D = \frac{r_\alpha r_\beta \rho_{\alpha\beta}}{\tau_r} (\mathbf{u}_\beta - \mathbf{u}_\alpha), \quad (3)$$

with the relaxation time defined as a fraction of the numerical time step $\tau_r = 10^{-8} \Delta t$ and mixture density $\rho_{\alpha\beta} = (r_\alpha \rho_\alpha + r_\beta \rho_\beta) / (r_\alpha + r_\beta)$.

As noted in the literature [11, 12, 13, 14], the prediction of flow fields near the gas-liquid interface in RANS simulations of stratified flows can be improved with the use of the turbulence damping approach [11]. Following previous work [14], the asymmetric approach is used, i.e. only the air turbulence is dampened. The turbulence damping term based on the damping scale δ formulation [13][14] is added into the transport equation for the specific dissipation rate of air turbulence, ω_g

$$S_g^\omega = Ar_g\beta\rho_g \left(\frac{\nu_g}{\beta\delta^2} \right)^2. \quad (4)$$

The terms in Eq. (4) are: A interface indicator field, r_g gas volume fraction, β one of the coefficients of the k - ω SST model, and $\nu_g = \mu_g/\rho_g$ the kinematic viscosity of gas. The damping scale was set to $\delta = 7 \cdot 10^{-5}$ m, as suggested in [14]. The turbulence damping is applied only near the gas-liquid surface with non-zero values of the interface indicator field, which is defined as

$$A = \min(a_{\alpha\beta}\Delta, 1), \quad a_{\alpha\beta} = |r_\beta \nabla r_\alpha - r_\alpha \nabla r_\beta|, \quad (5)$$

where $a_{\alpha\beta}$ is the interfacial area density, and Δ is the characteristic local cell size.

2.2 Computational domain and setup

The test section of the WENKA channel [6] is approximated with a two-dimensional computational domain as shown in Fig. 1. Simulations are performed using five hexahedral meshes with increasing level of refinement, as indicated by the number and prescribed sizes of cells given in Tab. 1.

Previous works in the literature [12, 13, 14] considered a smooth gas-liquid interface in the supercritical stratified flow regime. In contrast, the flow and boundary conditions (shown in Tab 2) used for the validation of present simulations are based on the measurement runs 2 and 22 of the WENKA experiment [6] in the partial flow reversal regime with significant liquid waves.

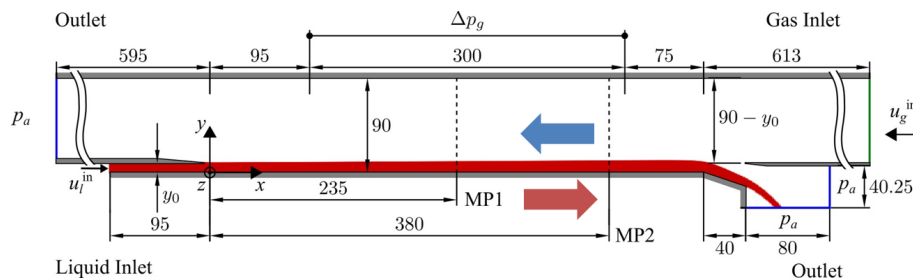


Figure 1: Computational domain with boundary conditions representing the test section of WENKA channel. All dimensions are in mm.

Fully developed flow is assumed for both gas and liquid inlets. Inlet profiles for the velocity and turbulence fields are obtained with a field mapping approach, as solely the average bulk velocities are available from the experiment (see Tab. 2). At the channel walls no-slip boundary conditions are prescribed. The pressure is set to a constant value at both outlet boundaries (top-left and bottom-right in Fig. 1), while the zero-gradient condition is set for all the other fields in those locations.

Table 1: Different mesh refinements with cell sizes for the channel section.

	Δx [mm]	Δy_{water} [mm]	Δy_{air} [mm]	N_{cells} [–]
Mesh 1	5.00	1.00	2.60	8002
Mesh 2	2.50	0.50	1.30	32557
Mesh 3	1.25	0.25	0.65	130528
Mesh 4	0.625	0.125	0.325	524317
Mesh 5	0.3125	0.0625	0.1625	2097742

Table 2: Fluid properties and flow conditions

	ρ_{α} [kg/m ³]	μ_{α} [Pa · s]	u_{α}^{in} [m/s]	Re_{α} [–]
Air (<i>g</i>)	1.20	$1.82 \cdot 10^{-5}$	10.0	$6.15 \cdot 10^4$
Water (<i>l</i>)	998	$1.00 \cdot 10^{-3}$	0.279	$4.64 \cdot 10^3$

Equations are solved with the PISO pressure-velocity coupling method. The accuracy of discretization schemes is second order in space and first order in time. The interface compression method [15] is used to limit the numerical smearing of the simulated gas-liquid interface. The size of the numerical time step is adapted, such that the maximum Courant number takes a value of 0.5. After simulating the initial transient for 10 s, the unsteady flow with periodic liquid waves on the surface is averaged over additional 10 s to obtain the mean fields that are presented in the results.

3 RESULTS AND DISCUSSION

In the partial flow reversal regime, the flow of water entering at the liquid inlet, and flowing through the channel, is partially reversed by the counter-current flow of gas coming from the gas inlet on the right (see Fig. 1), with the formation of periodic surface waves. As a result the water splits up: one part leaves the channel over a ramp at the bottom-right, while the remaining part exits the domain with the co-current flow of gas to the outlet on the left side.

Results presented in Fig. 2 show the distribution of water in the channel at the end of simulation and demonstrate the apparent necessity for a special treatment of turbulence near the gas-liquid interface. As shown in Fig. 2a, without the interfacial turbulence damping term from Eq. (4) the simulated flow of water is fully reversed resulting in the dry-out phenomena in the channel, which is not observed in the experiment [6]. Results without turbulence damping indicate an over-prediction in the modelled momentum transfer between gas and liquid at the interface. Present observations are similar to previous works on the supercritical stratified flow regime with smooth gas-liquid interface [12, 14]; without turbulence damping a qualitatively different flow regime is predicted.

Next, the flow reversal rate (FRR) can be defined as

$$\text{FRR} = \left| \frac{\dot{m}_l^{\text{reversed}}}{\dot{m}_l^{\text{inlet}}} \right|, \quad (6)$$

where \dot{m}_l^{inlet} is the liquid inlet flow, and $\dot{m}_l^{\text{reversed}}$ is the flow of reversed liquid exiting through the left outlet boundary (see Fig. 1), co-current with the flow of gas in the channel. Figure 3 shows the flow reversal rate resulting from different mesh refinements compared with the experimental value [6].

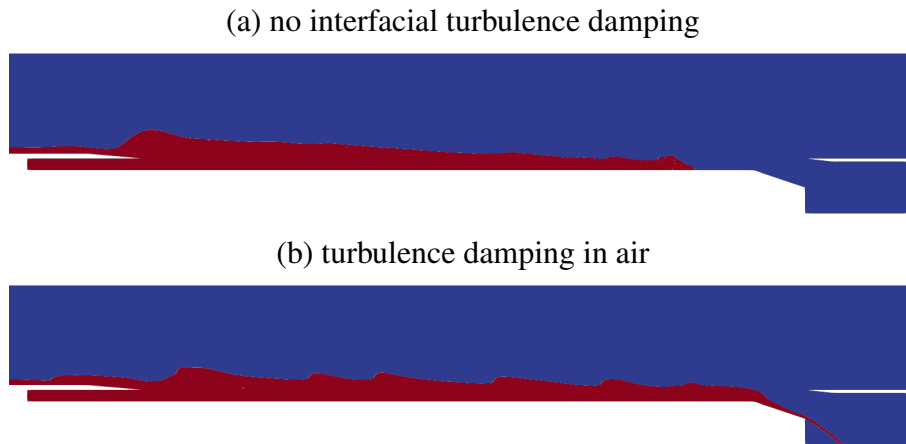


Figure 2: Distribution of water in the channel at the end of simulation ($t = 20$ s) on Mesh 5 without (a) and with (b) interfacial turbulence damping.

On the coarser meshes, 1 and 2, the gas-liquid interaction seems to be overestimated resulting in more flow reversal compared to the experiment. FRR significantly reduces with mesh refinement and by coincidence the result using Mesh 3 matches the experimental results. Finally, mesh convergence can be observed with the finest two meshes, 4 and 5, where the flow reversal is slightly under-predicted (by approx. 20%), which can be attributed to modelling errors other than discretization.

The aforementioned results quantitatively show that the momentum coupling between the two phases is over-predicted on coarse meshes, possibly due to numerically under-resolved description of the flow (e.g. velocity gradients) near the gas-liquid interface. Additional interphase drag modelling [16], e.g. one which allows for a less strict coupling (and thus a velocity slip) between phases at the interface, was not considered in the present work. The focus is rather on the examination of the effects of turbulence damping and mesh resolution itself.

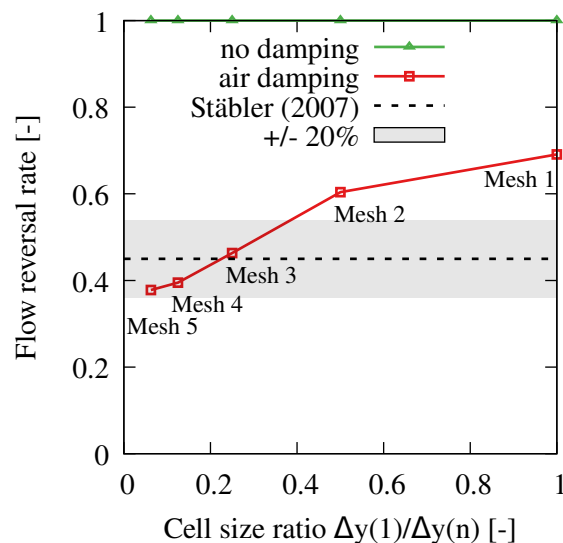


Figure 3: Flow reversal rate simulated with different meshes compared to the measured value [6]. The abscissa shows the cell size refinement relative to the coarsest Mesh 1. Without interface turbulence damping (green line) all of the liquid flow in the channel is reversed.

The last set of results is shown in Fig. 4 and compares the vertical profiles of air volume fraction, phase velocities, U_x , and mixture turbulent kinetic energy, k_m , measured at both two stream-wise positions (marked as MP1 and MP2 in Fig. 1) in the WENKA experiment [6] to the ones obtained with sampling of the time averaged fields in the present simulation. The first observation in Fig. 4 is that mesh convergence is obtained with the finest meshes, 4 and 5. At the same time, results show the average liquid height, indicated at an air volume fraction of 0.5, is over-predicted by approximately the same amount in all simulations. Again this hints that the discretisation related errors are not the main contribution to the discrepancies.

For comparison of velocity and turbulent kinetic profiles, the mixture fields are used, which are defined as

$$U_x = r_g u_{xg} + r_l u_{xl} \quad k_m = r_g k_g + r_l k_l, \quad (7)$$

where u_{xg} and u_{xl} are the stream-wise velocity components, and k_g and k_l are the turbulent kinetic energies of gas (g) and liquid (l), respectively. In fact, simulated gas and liquid velocities are identical ($\mathbf{u}_g = \mathbf{u}_l$), due to the strong drag coupling in the model. Therefore, the mixture velocity is also equal to $U_x = u_{xg} = u_{xl}$ (note also that $r_g + r_l = 1$).

Velocity profiles are shown in second and third row of Fig. 4 for the whole channel and in detail for the water section, respectively. Results generally show a good agreement with measured velocities. Slight deviations are observed right above liquid surface between the measured mean liquid and wave heights in the experiment [6]. Profiles of turbulent kinetic energy k_m are compared in the last row of Fig. 4 with a semi-log abscissa for convenience. Similarly to velocities, the simulated profiles agree well with the measured ones, except for the region right above the gas-liquid surface, where waves are present.

4 CONCLUSIONS

This work demonstrates the capability of *OpenFOAM-Hybrid* to simulate turbulent counter-current stratified flow regime with partial flow reversal and significant liquid waves. Results indicate that interface turbulence damping is required to obtain the correct flow regime. The mesh convergent results show a reversed flow rate of about 20% below the experimental value. The simulated liquid height is over-predicted. Stream-wise velocities and turbulent kinetic energy agree with the measurements, except in the region above the surface where waves are present. Further investigations are needed to reveal the nature of described discrepancies and to improve the simulation results.

Next steps in the model development for stratified flows might focus on an adaptive interphase drag modelling approach to improve predictions on coarser mesh resolutions. Future work could also consider applications with droplet and bubble entrainment, e.g. during wave breakup events, using a multi-field approach with additional dispersed phases.

ACKNOWLEDGMENTS

This work was supported by the Helmholtz European Partnering Program in the project ‘‘Crossing borders and scales (Crossing)’’. The author from Jožef Stefan Institute gratefully acknowledges financial support provided by the Slovenian Research Agency through the grant P2-0026.

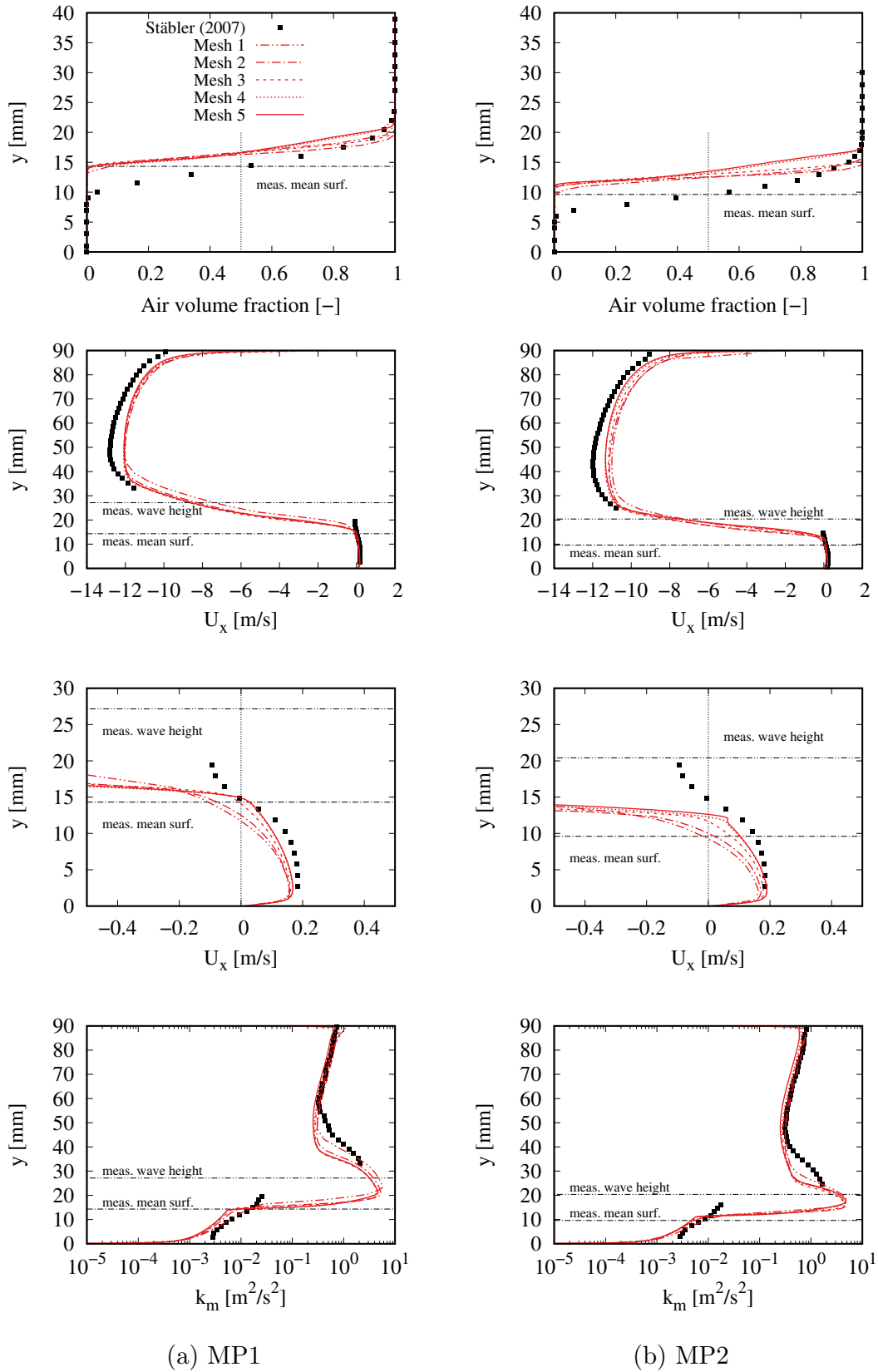


Figure 4: Vertical profiles of air volume fraction, stream-wise velocity U_x and turbulent kinetic energy k_m compared to measured values at the two stream-wise locations MP1 and MP2 in the experiment [6].

REFERENCES

- [1] Lucas, D., Bestion, D., Bodèle, E., Coste, P., Scheuerer, M., D'Auria, F., Mazzini, D., Smith, B., Tiselj, I., Martin, A., Lakehal, D., Seynhaeve, J.-M., Kyrki-Rajamäki, R., Ilvonen, M., and Macek, J., 2009. “An overview of the pressurized thermal shock issue in the context of the NURESIM project”. *Science and Technology of Nuclear Installations*, **2009**, pp. 1–13.
- [2] Kirsner, W., 1999. “Steam condensation induced waterhammer”. *HPAC Heating / Piping / Air-Conditioning*, **71(1)**, 01, p. 112–124.
- [3] Deendarlianto, Höhne, T., Lucas, D., and Vierow, K., 2012. “Gas–liquid countercurrent two-phase flow in a PWR hot leg: A comprehensive research review”. *Nuclear Engineering and Design*, **243**, feb, pp. 214–233.
- [4] Meller, R., Schlegel, F., and Lucas, D., 2020. “Basic verification of a numerical framework applied to a morphology adaptive multifield two-fluid model considering bubble motions”. *International Journal for Numerical Methods in Fluids*, **93(3)**, pp. 748–773.
- [5] Schlegel, F., Bilde, K. G., Draw, M., Evdokimov, I., Hänsch, S., Kamble, V. V., Khan, H., Krull, B., Lehnigk, R., Li, J., Lyu, H., Meller, R., Petelin, G., and Tekavčič, M., 2022. HZDR Multiphase Addon for OpenFOAM (version 9-s.1-hzdr.2). Rodare. <http://doi.org/10.14278/rodare.1742>.
- [6] Stäbler, T. D., 2007. “Experimentelle untersuchung und physikalische beschreibung der schichtenströmung in horizontalen kanälen”. PhD thesis, Universität Stuttgart.
- [7] Ishii, M., and Hibiki, T., 2006. *Thermo-Fluid Dynamics of Two-Phase Flow*. Springer US.
- [8] Menter, F. R., Kuntz, M., and Langtry, R., 2003. “Ten years of industrial experience with the SST turbulence model”. *Turbulence, Heat and Mass Transfer*, **4**, pp. 625–632.
- [9] Brackbill, J. U., Kothe, D. B., and Zemach, C., 1992. “A continuum method for modeling surface tension”. *Journal of Computational Physics*, **100(2)**, jun, pp. 335–354.
- [10] Štrubelj, L., and Tiselj, I., 2010. “Two-fluid model with interface sharpening”. *International Journal for Numerical Methods in Engineering*, **85(5)**, dec, pp. 575–590.
- [11] Egorov, Y., 2004. Validation of cfd codes with pts-relevant test cases. Tech. rep., EVOL-ECORA-D07, pp. 102–115.
- [12] Porombka, P., and Höhne, T., 2015. “Drag and turbulence modelling for free surface flows within the two-fluid euler–euler framework”. *Chemical Engineering Science*, **134**, sep, pp. 348–359.
- [13] Frederix, E., Mathur, A., Dovizio, D., Geurts, B., and Komen, E., 2018. “Reynolds-averaged modeling of turbulence damping near a large-scale interface in two-phase flow”. *Nuclear Engineering and Design*, **333**, jul, pp. 122–130.
- [14] Tekavčič, M., Meller, R., and Schlegel, F., 2021. “Validation of a morphology adaptive multi-field two-fluid model considering counter-current stratified flow with interfacial turbulence damping”. *Nuclear Engineering and Design*, **379**, aug, p. 111223.

- [15] Weller, H. G., 2008. A new approach to VOF-based interface capturing methods for incompressible and compressible flow. Tech. rep., OpenCFD Ltd., Report TR/HGW.
- [16] Meller, R., Krull, B., Schlegel, F., and Tekavčič, M., 2021. “Classification and resolution adaptive drag modelling of gas-liquid interfaces with a multifield two-fluid model”. In Proceedings of the International Conference Nuclear Energy for New Europe (NENE2021), Bled, Slovenia, September 6–9.